Archival Report

Biological Psychiatry: GOS

Stress History Modulates Corticotropin-Releasing Factor Neurons to Establish Resilience

Sherod E. Haynes, Anthony Lacagnina, Hyun Seong Seo, Fang Li, Xiao Yang, Muhammad Furqan Afzal, Carole Morel, Aurelie Menigoz, Kanaka Rajan, Roger L. Clem, Barbara Juarez, Helen S. Mayberg, Donald G. Rainnie, Larry J. Young, and Ming-Hu Han

ABSTRACT

BACKGROUND: Cumulative stress is a major risk factor for developing major depressive disorder (MDD), but not everyone experiencing chronic stress develops MDD. In those who do not, it is unclear at what point or by what mechanism a trajectory of stable resiliency emerges.

METHODS: Utilizing a 10-day repeated social defeat stress (RSDS) model for MDD, we observed that a critical period between 7 and 10 daily defeats marks the phenotypical divergence of resilient from susceptible male mice. Cell-type selective electrophysiology, chemogenetics, optogenetics, and RNA quantification were used to investigate the nature of stress effects on neuroadaptation in the oval nucleus of the bed nucleus of the stria terminalis (BNSTov) required to determine resilience.

RESULTS: In response to ongoing stress, corticotropin-releasing factor (CRF^{+}, but not CRF^{-}) neurons of the BNSTov displayed a sustained increased firing rate in resilient but not susceptible mice. This neurophysiological adaptation was self-sustaining, but only after 7 critical stress exposures, indicating that the process of developing resilience is dependent on stress history.

CONCLUSIONS: Our study reveals a novel process by which individuals may persist in the face of adversity by way of stress-provoked activation, not inhibition of a key CRF limbic region that establishes a pathway to resilience.

https://doi.org/10.1016/j.bpsgos.2025.100656

Major depressive disorder (MDD) is a crippling, heterogeneous neuropsychiatric condition with high morbidity and lifetime prevalence (1,2). Major life stressors are key precipitants in the onset of an episode (3,4). Cumulative stress causes numerous psychological insults that predispose people to neuropsychiatric conditions (5–7). Many studies have explored individual differences in stress susceptibility or resiliency, but the process critical to driving the divergence in phenotypes remain elusive. With the odds of treatment failure increasing with subsequent depressive episodes (2,8,9) and increased depression risk associated with cumulative stress, a potentially more effective strategy would be to target the mechanisms mediating resilience, thereby enhancing the ability to cope with cumulative stress.

Resiliency is defined as the "process of adapting well in the face of adversity, threats, or significant sources of stress" (10–12). Repeated social defeat stress (RSDS) induces robust depression-like behavioral phenotypes in approximately two-thirds of mice (7,13). The standard 10-day RSDS protocol has been widely used to identify and study neurobiological features of susceptible and resilient subpopulations (13–21). Studies on stress vulnerability often test hypotheses after establishing vulnerable subgroups, making the processes that led to such phenotypic diversification unclear.

The bed nucleus of the stria terminalis (BNST) is well positioned in the social salience network to integrate external cues with internal states to influence the outcome and context of social interactions (22–25). The oval nucleus of the BNST (BNSTov) is a stress-sensitive subregion that is a key candidate region for encoding stress modulation of social behavior through its projections to areas such as the ventral tegmental area (VTA) (26–29) and dorsal raphe (30,31). Corticotrophin-releasing factor (CRF) neurons of the BNSTov ($BNSTov^{CRF}$) are a significant output of this region and can influence affective states (32–35). CRF receptor type 1 (CRFR1) has been confirmed to be distributed on $BNSTov^{CRF}$ neurons, and CRFR1-mediated hyperexcitation of these $BNSTov^{CRF}$ neurons has been shown to encode female-biased susceptibility to anxiety (36). Since $BNSTov^{CRF}$ neurons are thought to promote arousal and adaptive responding according to stress-related changes in internal state (22,23,25,37–43), we hypothesized that they may play a role in establishing resiliency to repeated social stress.

With the 10-day RSDS paradigm, we used cell-type–selective ex vivo electrophysiology, chemogenetics, optogenetics, and in vivo fiber photometry to interrogate the $BNSTov^{CRF}$ system to explore its role in the divergence of susceptible and resilient

ISSN: 2667-1743

phenotypes. Unexpectedly, we observed that resiliency entails cumulative stress history–dependent neuroadaptive changes, whereas susceptibility emerges in the absence of similar adaptations. Activation of BNSTov^{CRF} neurons using DREADDs (designer receptors exclusively activated by designer drugs) during social defeat led to a resilient phenotype while inhibition caused susceptibility. Finally, using RNAScope and optogenetics, we provided intriguing evidence for a potential role of *Crfr1* in BNSTov^{CRF} neurons in mediating resilience.

METHODS AND MATERIALS

Mice

The study used male, wild-type, Crf-ires-Cre (Jackson Labs: 011087), ai14 (Cre-responsive tdTomato reporter mouse; Jackson Labs: 007915), ai32 (Cre-responsive ChR2 [channelrhodopsin-2]/fused with eYFP [enhanced yellow fluorescent protein]; Jackson Labs: 012569) mice on C57BL/6J background that were bred at the Icahn School of Medicine at Mount Sinai (ISMMS) and were used between 6 and 7 weeks at the start of experimental manipulations. All experiments were approved by the Institutional Animal Care and Use Committee and comply with institutional guidelines for the Animal Care and Use Committee set forth by ISMMS.

RSDS Paradigm

The RSDS paradigm was performed according to published protocols (6,19,21,44–47). Briefly, CD1 aggressors were singly housed in cages (26.7 cm width × 48.3 cm depth × 15.2 cm height; Allentown Inc.) at least 24 hours before the start of the experiment on one side with a clear perforated Plexiglas divider. Social stress consists of physical and sensory stress components.

Viral Constructs

For DREADD experiments in CRF neuronal populations, CRF-ires-Cre animals were injected with AAV5-hSyn-DIO-hM4D(Gi)-mCherry (Addgene: 44362-AAV5) (≥7 trillion), AAV5-hSyn-DIO-hM3D(Gq)-mCherry (Addgene: 44361-AAV5) (≥7 trillion), and AAV5-hSyn-DIO-mCherry (Addgene: 50459). For fiber photometric recordings, CRF-ires-Cre animals were injected with AAV9-syn-FLEX-jGCaMP7f-WPRE (Addgene: 104492-AAV9) (>1 trillion). All viruses were purchased from Addgene.

Clozapine *N*-Oxide Drinking Water Construct

Clozapine *N*-oxide (CNO) was obtained from Hello Bio (cat. # HB6149). The dry chemical was dissolved in drinking water obtained from the vivarium and diluted such that each mouse received 5 mg/kg/day based on previous studies. CNO was made fresh each day for the 3 days it was administered. CNO solutions were protected from light throughout the experimental procedure. On average, mice consumed approximately 4 to 5 mL of water per day. Water bottles and mice were weighed daily.

Please see the Supplemental Methods for further details.

Statistical Analysis

Animals were randomly assigned to control and experimental groups, and all experimenters were blinded. Mice were excluded if viral infection was off target. No data were excluded for other reasons. Two-tailed Student's *t* tests were used for comparisons of 2 experimental groups. For parametric datasets, comparisons among 3 or more groups were performed using one or two-way ANOVAs followed by Tukey's or Bonferroni post hoc tests. For all tests, $p < .05$ was the cutoff for significance. Statistical analyses were performed using GraphPad Prism version 9.3.1 software. For data not normally distributed, nonparametric analyses were performed.

RESULTS

Susceptible Versus Resilience Phenotypes Emerge Between 7 and 10 Daily Episodes of SDS

RSDS produces divergent and enduring resilient/susceptible phenotypes following 10 episodes of SDS (6,19) and enables the investigation of the consequences of stress accumulation (5,7). To examine the temporal divergences of resilient and susceptible phenotypes in mice, a modified RSDS protocol was used in which mice were subjected to discrete numbers of social defeat episodes (SDEs) interspersed with social interaction (SI) and sucrose preference (SP) tests administered after 1, 4, 7, and 10 SDEs (Figure 1A–D). The SI ratio is a behavioral score of the SI test and measures the time spent in the area proximal to the enclosure of a novel social target (SI zone) (19).

Surprisingly, we found that the susceptible phenotype emerged discretely between 7 and 10 SDEs (Figure 1E and Figure S1A) (SI ratio: 2.062 ± 0.226 after 7 SDEs to 0.559 ± 0.093, $p < .0001$, $n = 11$ for susceptible and 1.967 ± 0.188 [7 SDEs] to 1.554 ± 0.163 [10 SDEs], $p = .2929$, $n = 11$ for resilient). There were no significant differences in SI ratios after 7 SDEs between mice that went on to become susceptible versus resilient after 10 SDEs (mean: 2.062 ± 0.226 vs. 1.967 ± 0.188, two-tailed *t* test, $p = .7483$, $n = 11$/group) (Figure S1B, C). This effect was not due to repeated SI tests (Figure S2D–F). Resilient mice had an indistinguishable SI ratio from all mice after 7 SDEs, while susceptible (10 SDEs) mice had an SI ratio significantly lower than both groups (Figure 1F, G). Previous studies reported that RSDS produces susceptible and resilient phenotypes after 10 SDEs in a bimodal distribution (19). Here, we observed a unimodal distribution of social interaction toward a novel conspecific in 7-SDE mice but a bimodal distribution in 10-SDE mice, consistent with the emergence of distinct resilience and susceptible phenotypes (Kolmogorov-Smirnov, $p < .0001$) (Figure 1H–J). The time spent interacting with a novel conspecific was significantly less in susceptible 10-SDE mice compared with the 7-SDE and 10-SDE resilient mice, which were indistinguishable (Figure 1K). The phenotypic divergence was dependent on the number of SDEs rather than the passage of time and dependent upon the anterior dorsal BNST (Figures 1G and 2A–E).

Divergence in BNSTov^{CRF} Neuronal Firing Rate Tracks the Emergence of Resilient and Susceptible Phenotypes

CRF neurons of the BNST are a major output source of the BNSTov that are sensitive to chronic stressors (25,48–50). Thus, we hypothesized that chronic stress would alter

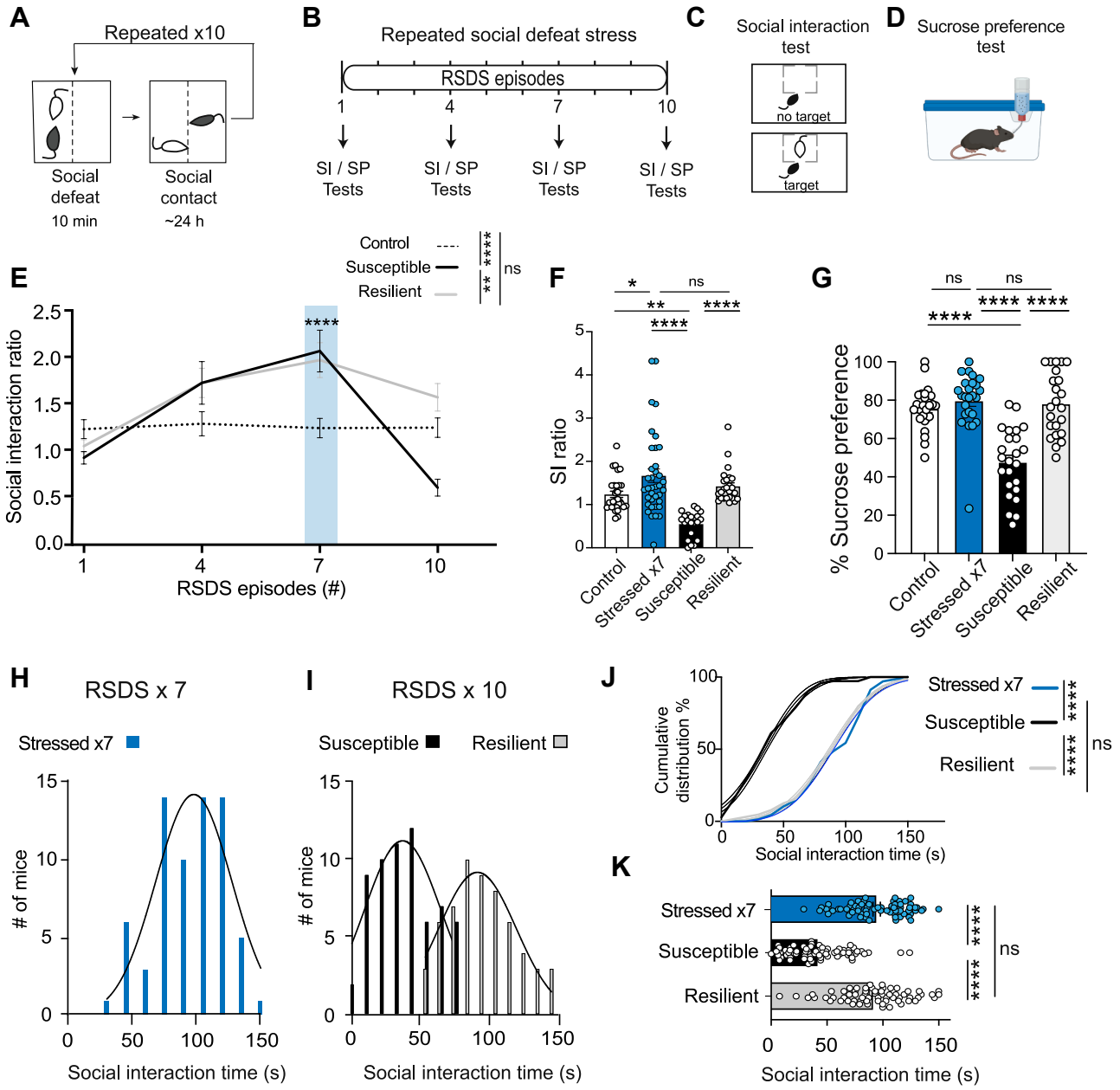

Figure 1. Susceptible and resilient subgroups emerge between 7 and 10 daily episodes of SDS. **(A)** Experimental design for RSDS. **(B)** Experimental timeline of SDS and behavioral tests: SI and SP. **(C)** SI test schema involving target and no-target trials. **(D)** SP test schematic. **(E)** Effect of cumulative SDS on social interaction measured as SI ratios after 1, 4, 7, and 10 SDEs (n = 11–18 mice/group), two-way ANOVA interaction $F_{6,134} = 5.783$, ****$p < .0001$, row factor $F_{3,134} = 12.11$, ****$p < .0001$, column factor $F_{2,134} = 4.086$, *$p < .05$; Tukey's post hoc test susceptible vs. resilient ****$p < .0001$, susceptible vs. control **$p < .01$, resilient vs. control $p = .2751$. SI test susceptible (SI test stressed ×7 vs. stressed ×10) ****$p < .0001$. **(F)** Aggregated data on SI test across experiments. One-way ANOVA treatment $F_{3,109} = 14.61$, ****$p < .0001$. Tukey's post hoc test control vs. stressed ×7 *$p < .05$, control vs. susceptible **$p < .01$, stressed ×7 vs. susceptible ****$p < .0001$, susceptible vs. resilient ****$p < .0001$ (n = 25–37 mice). **(G)** SP test. One-way ANOVA treatment $F_{3,93} = 24.06$, ****$p < .0001$. Tukey's post hoc test control vs. stressed ×7 $p = .77$, control vs. susceptible ****$p < .0001$, control vs. resilient $p = .9387$, stressed ×7 vs. susceptible ****$p < .0001$, stressed ×7 vs. resilient $p = .984$, susceptible vs. resilient ****$p < .0001$ (n = 23–25 mice). **(H)** Distribution of stressed mice that underwent 7 SDEs. **(I)** Distribution of mice that underwent 10 SDEs sorted into susceptible and resilient mice. **(J)** Cumulative distribution of all stressed mice. Kolmogorov-Smirnov (distance) 0.2054, susceptible vs. resilient ****$p < .0001$. **(K)** Time spent interacting socially with a novel conspecific. One-way ANOVA $F_{2,201} = 76.63$, ****$p < .0001$. Tukey's post hoc susceptible vs. resilient ***$p < .001$, susceptible vs. stressed ×7 ****$p < .0001$, stressed vs. resilient $p = .4984$ (n = 72 susceptible, 64 resilient mice). All data represent mean ± SEM. *$p < .05$, **$p < .01$, ***$p < .001$, ****$p < .0001$. ANOVA, analysis of variance; ns, not significant; RSDS, repeated social defeat stress; SDE, social defeat episode; SI, social interaction; SP, sucrose preference.

BNSTov^{CRF} neuronal activity, coinciding with the divergence in resilient and susceptible behavioral phenotypes. To test this hypothesis, Crf-ires-Cre;ai14 (tdTomato) mice (28,51–54) were subjected to either 7 or 10 daily SDEs, and cell-attached ex vivo electrophysiological recordings were conducted in the BNSTov (Figure 2A, B). CRF^{+}, but not CRF^{-}, BNSTov neurons of 7-SDE mice had significantly increased firing rates compared with stress-naïve control mice. CRF^{-} neuronal

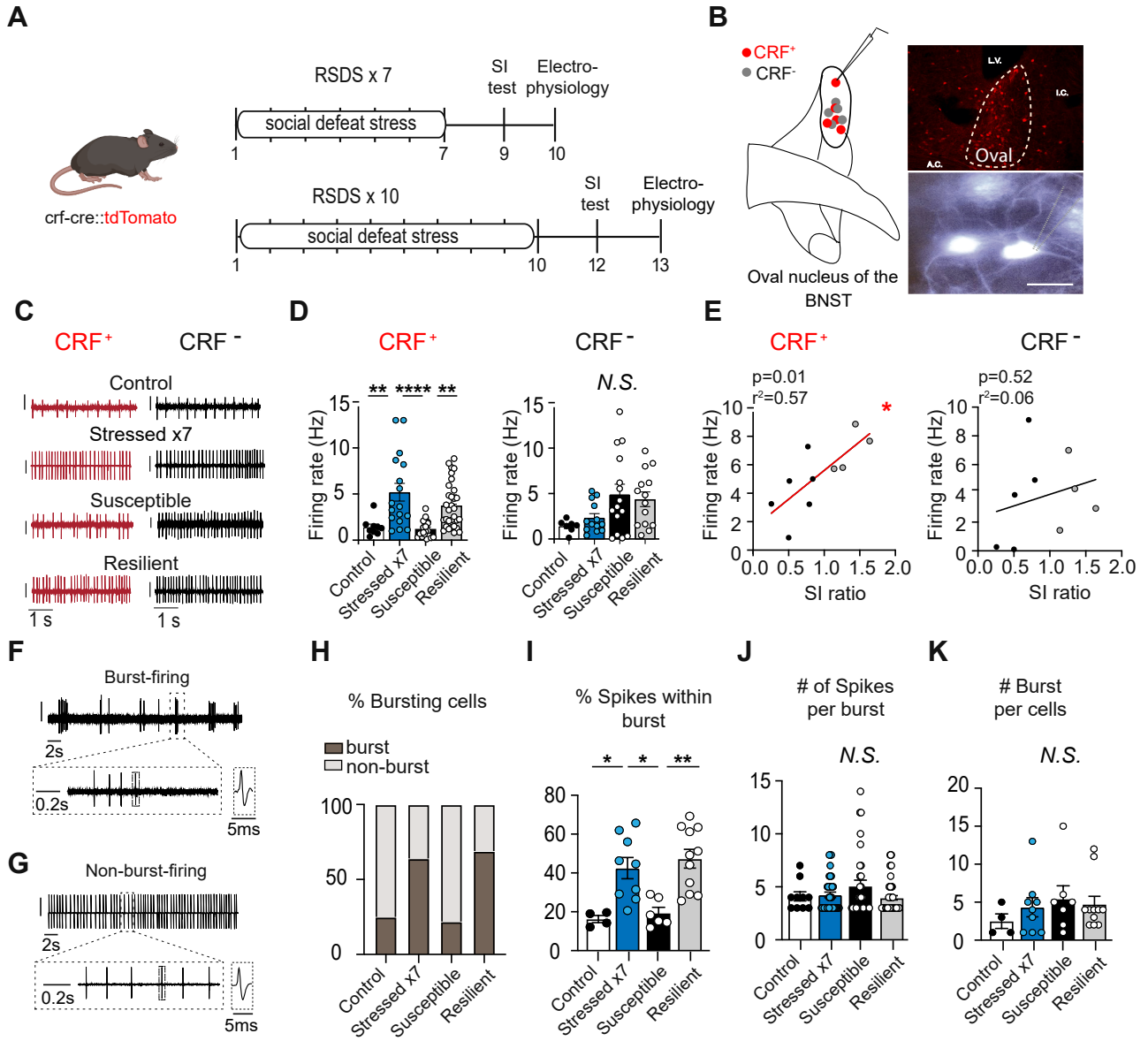

Figure 2. Firing rate alterations in BNSTovCRF neurons occur as adaptation to social stress, persisting in resilient but not susceptible mice. **(A)** Mouse genotype and timeline of cell-attached electrophysiology experiments. **(B)** Fluorescence-guided cell-attached electrophysiology setup, brain slice of the BNST (CRF cells, tdTomato) and DIC image of CRF neurons; scale bar 0.63 mm. **(C)** Representative trace of BNSTovCRF-positive and negative neurons of control, stressed (SDEs × 7), susceptible, and resilience mice. **(D)** Firing rate of CRF^{+} neurons (n = 9–31 cells/group), ****$p < .0001$, one-way ANOVA, Tukey's multiple comparison's test, control vs. stressed (SDEs × 7) **$p < .01$, susceptible vs. resilient **$p < .01$, susceptible vs. stressed (SDEs × 7) ****$p < .0001$. Firing rate of CRF^{-} neurons (n = 7–15 cells per 4–6 mice/group), one-way ANOVA, $F_{3,45} = 3.113$, *$p < .05$, Tukey's multiple comparison's test, control vs. stressed ×7 $p = .9192$, control vs. susceptible $p = .0769$, control vs. resilient $p = .1742$, stressed (SDEs × 7) vs. susceptible $p = .1370$, stressed ×7 vs. resilient $p = .3219$, susceptible vs. resilient $p = .9673$. **(E)** Correlation of firing rate with social interaction ratio: CRF^{+}, $R^2 = 0.5726$, *$p < .05$; CRF^{-}, $R^2 = 0.0609$, $p = .5219$. **(F)** Representative sample of burst firing. **(G)** Representative sample of tonic firing. **(H)** Percentage of bursting cells per animal group. **(I)** Percentage of spikes within burst. **(J)** Number of spikes per burst. **(K)** Number of bursts per cell. (n = 10–52 cells per 4–6 mice/group). All data represent mean ± SEM. *$p < .05$, **$p < .01$, ***$p < 0.001$, ****$p < .0001$. ANOVA, analysis of variance; BNSTov, oval nucleus of the bed nucleus of the stria terminalis; CRF, corticotropin-releasing factor; DIC, differential interference contrast; ns, not significant; SDE, social defeat episode.

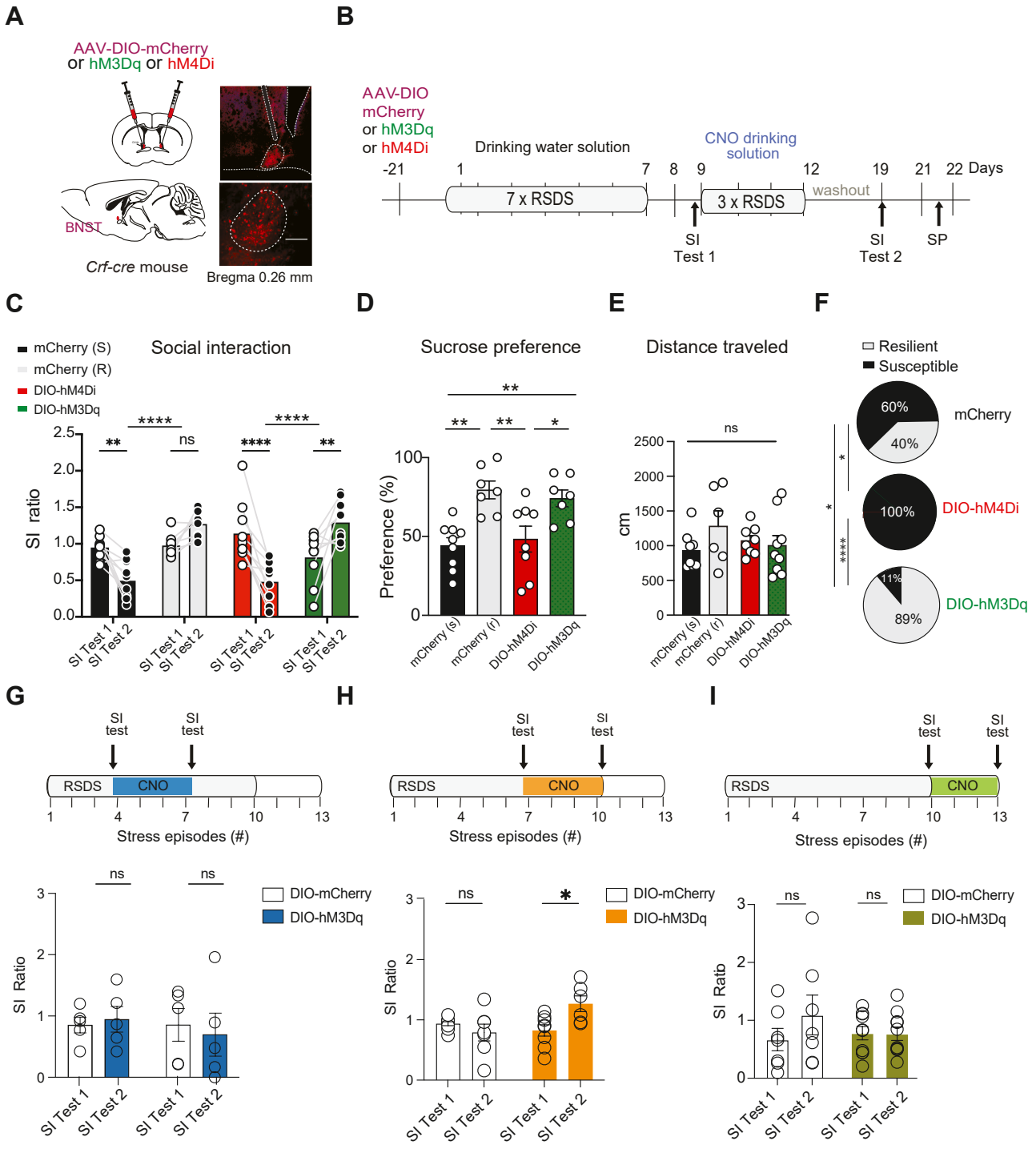

Figure 3. Chemogenetic modulation of BNSTovCRF neurons bidirectional recapitulates behavioral tipping point. **(A)** Viral targeting of the BNSTov. **(B)** Experimental design of chemogenetic manipulation of BNSTov neurons with CNO-drinking water construct. **(C)** SI test, two-way ANOVA $F_{3,68} = 18.01$, row $^{****}p < .0001$, row factor $F_{3,68} = 9.965$, $p = .2616$ (time), row factor × time $F_{1,68} = 1.281$, $^{****}p < .0001$, Sidak's multiple comparisons test mCherry (S), $^{**}p = .0017$ ($n = 10$ mice); mCherry (R), $p = .1322$ ($n = 9$ mice); hM4Di, $^{****}p < .0001$ ($n = 10$ mice); hM3Dq, $^{**}p = .0018$ ($n = 9$ mice). **(D)** SP test. One-way ANOVA treatment $F_{3,27} = 8.310$, $^{***}p < .001$, Tukey's post hoc testing susceptible vs. hM4Di, $p = .9619$; susceptible vs. resilient, $^{**}p < .01$; susceptible vs. hM3Dq, $^{**}p < .01$; hM4Di vs. resilient, $^{**}p < 0.01$; hM4Di vs. hM3Dq, $^{*}p < .05$; resilient vs. hM3Dq, $p = .9368$ (7–9 mice per group). **(E)** Distance traveled, one-way ANOVA $F_{3,27} = 1.031$, $p = .3944$. **(F)** Percentage of susceptible or resilient mice: DIO-hM4Di, 100% susceptible; DIO-hM3Dq, 89% resilient and 11% susceptible; mCherry, 40% resilient and 60% susceptible. $\chi^2_2 = 15.66$, $^{***}p < .001$ ($n = 21$ mCherry, 10 hMDi, 9 hM3Dq); Fisher's post hoc test mCherry vs. hM4Di, $^{*}p < .05$; mCherry vs. hM3Dq, $^{*}p < .05$; hM4Di vs. hM3Dq, $^{****}p < .0001$. **(G)** Repeated social defeat DREADDs manipulation (4–7 episodes of stress), two-way ANOVA treatment $F_{1,16} = 0.01749$, $p = .8964$; SI test 1 vs. SI test 2, $F_{1,16} = 0.2377$, $p = .6325$; interaction

firing did not differ between groups (Figure 2C, D). Moreover, there was a strong correlation between firing rate and the SI ratio in CRF^+ but not CRF^- neurons in 10-SDE mice (CRF^+, $R^2 = 0.5725$, $^*p = .0113$; CRF^- $R^2 = 0.06096$, $p = .5219$) (Figure 2E). CRF neurons display both burst and nonburst firing patterns (39,55,56) (Figure 2F). Burst firing patterns were prominent in resilient and 7-SDE mice compared with susceptible and control mice (Figure 2H). Additionally, percentage spikes within burst were higher in 7-SDE and resilient mice compared with susceptible 10-SDE mice (one-way analysis of variance [ANOVA], $p = .0004$) (Figure 2I) but not susceptible or control mice. The number of spikes per burst and number of bursts per cell were not significantly different between the groups (Figure 2J, K). These data and correlation analysis suggest the possibility that there is a causal link between the neuronal activity of $BNSTov^{CRF}$ neurons and the divergence of behavioral phenotypes.

$BNSTov^{CRF}$ Neurons Bidirectionally Modulate the Emergence of Resiliency

To test the hypothesis that $BNSTov^{CRF}$ neurons regulate and maintain resilience over the last 3 episodes of RSDS, we injected *Crf-ires-Cre* mice with AAVs (adeno-associated viruses) encoding Cre-dependent excitatory (DIO-hM3Dq), inhibitory (DIO-hM4Di) DREADDs, or mCherry construct (control) into the BNSTov and administered CNO via drinking water (57–59) (Figure 3A, B). The mCherry control mice exhibited both susceptible and resilient phenotypes (SI ratio <1.0 and ≥ 1.0, respectively) in approximately a 60:40 ratio as expected (6,19) (Figure 3C, F). Interestingly, mice injected with inhibitory DIO-hM4Di displayed a robust susceptible phenotype, while DIO-hM3Dq mice displayed resilient phenotypes following CNO drinking water administration (Figure 3C). Moreover, none of the DIO-hM4Di + CNO mice went on to develop resilience (0/10, SI > 1.0), while 89% (8/9, SI ≥ 1.0) of the DIO-hM3Dq mice were resilient (Figure 3C, F). Notably, the social defeat experience was not affected by the DREADD manipulations (Figure 3A, B). The SP test—a test of hedonic behavior—revealed differences between mCherry-susceptible (mCherry [S]) and resilient (mCherry [R]) mice that were mirrored in DIO-hM4Di and hM3Dq mice, respectively. mCherry (S) and hM4Di mice displayed a significant decrease in SP relative to mCherry (R)- and hM3Dq-injected mice (Figure 3D). There were no significant differences in locomotion (Figure 3E). The chemogenetic manipulation also produced bidirectional effects on anxiety-like behavior in elevated plus maze and open-field tests (Figure S4). Surprisingly, mice injected with hM3Dq DREADDs went on to become resilient (Figure 3C), although activation of *Crf* neurons of the BNST has previously been shown to produce depressive- and anxiogenic-like responses (25,32,38,49,52,60). Interestingly, resilience was established if $BNSTov^{CRF}$ chemogenetic activation occurred between 7 and 10 SDEs; excitatory hM3Dq DREADD activation during episodes 4 to 7 or 10 to 13 was not associated with resiliency (Figure 3G–I), suggesting that stress history plays a critical role in the behavioral outcomes of CRF modulation. Modulating *Crf* neurons with inhibitory hM4Di or excitatory hM3Dq DREADDs between 8 and 10 SDEs led to enduring susceptible or resilient phenotypes, respectively, up to 6 weeks after CNO manipulation (Figure S6). These observations strongly support that the behavioral outcomes induced by the activation of $BNSTov^{CRF}$ neurons are stress history dependent.

Calcium Dynamics Underlying Stress Adaptation

To draw a link between neural changes and behavior in vivo, we combined fiber photometry (gCAMP7f) with excitatory or inhibitory DREADDs (Cre-dependent -hM4Di, -hM3Dq DREADDs, or mCherry viral vectors) to mimic the neuroadaptive changes in $BNSTov^{CRF}$ neurons and bidirectionally drive the development of resilience/susceptibility (Figure 4A, B). CNO was administered via drinking water over the last 3 SDEs. We hypothesized that calcium-encoded neural activity may diverge in susceptible/resilient mice concomitant with the display of their respective behaviors on the SI test. When comparing changes in calcium-encoded neural dynamics between SI tests 1 and 2, mCherry (S) mice showed no difference, whereas mCherry (R) mice developed an increase concomitant with the display of resilience (Figure 4C–E), not observed in mice enduring only 7 SDEs. These findings suggest that the persistence of neural activity across SDEs 8 to 10 is associated with resiliency.

During SI test 1, similar to control mice, DREADDs-injected mice experienced a decrease in calcium-related neural activity upon initiating SI with a novel conspecific (Figure S7A), whose neural pattern was observed in both no-target and target trials (Figure S7B). In hM4Di-injected mice, there were no significant differences in neural activity during SI test 1 and 2 trials, similar to control mCherry (S) mice (Figure 4F–H and Figure S7A–C). As was observed in the resilient (mCherry [R]) mice, the hM3Dq-injected group showed an increase in calcium-encoded neural activity (Figure 4F–H). Mice injected with Cre-dependent hM4Di showed a significant decrease in calcium-related neural activity. In contrast, SI initiation led to increased activity in DIO-hM3Dq-injected mice (Figure 4F–H). There were no significant differences in the SI of mice subjected to 7 SDEs, but differences emerged following 3 additional SDEs, with a subset of mice becoming susceptible and resilient (mCherry[R]/[S]) or activating/inhibiting DREADD promoting resiliency and susceptibility in the direction predicted (Figure 4I). We observed a strong correlation between the SI ratio and calcium activity only after 10 SDEs (Figure 4J). There were no significant differences observed in calcium-based neuronal activity upon SI with a novel conspecific in

$F_{1,16} = 0.07055$, $p = .6218$ (n = 5–6 mice/group). **(H)** RSDS DREADDs manipulation (7–10 episodes of stress), two-way ANOVA treatment, $F_{1,22} = 8.675$, $^{**}p < .01$; SI test 1 vs. SI test 2, $F_{1,22} = 2.549$, $p = .1247$; interaction $F_{1,22} = 2.549$, $p = .1247$. Sidak's post hoc test SI test 1 vs. SI test 2, control, $p = .5533$; DIO-hM3Dq, $^*p < .05$ (n = 6–7 mice/group). **(I)** RSDS DREADDs manipulation (10–13 episodes of stress), two-way ANOVA treatment, $F_{1,30} = 1.192$, $p = .2623$. SI test 1 vs. SI test 2, $F_{1,30} = 0.3132$, $p = .2836$. Interaction $F_{1,30} = 0.2623$, $p = .5799$. All data represent mean ± SEM. $^*p < .05$, $^{**}p < .01$, $^{***}p < .001$, $^{****}p < .0001$. ANOVA, analysis of variance; BNSTov, oval nucleus of the bed nucleus of the stria terminalis; CNO, clozapine *N*-oxide; DREADD, designer receptors exclusively activated by designer drugs; ns, not significant; RSDS, repeated social defeat stress; SI, social interaction; SP, sucrose preference.

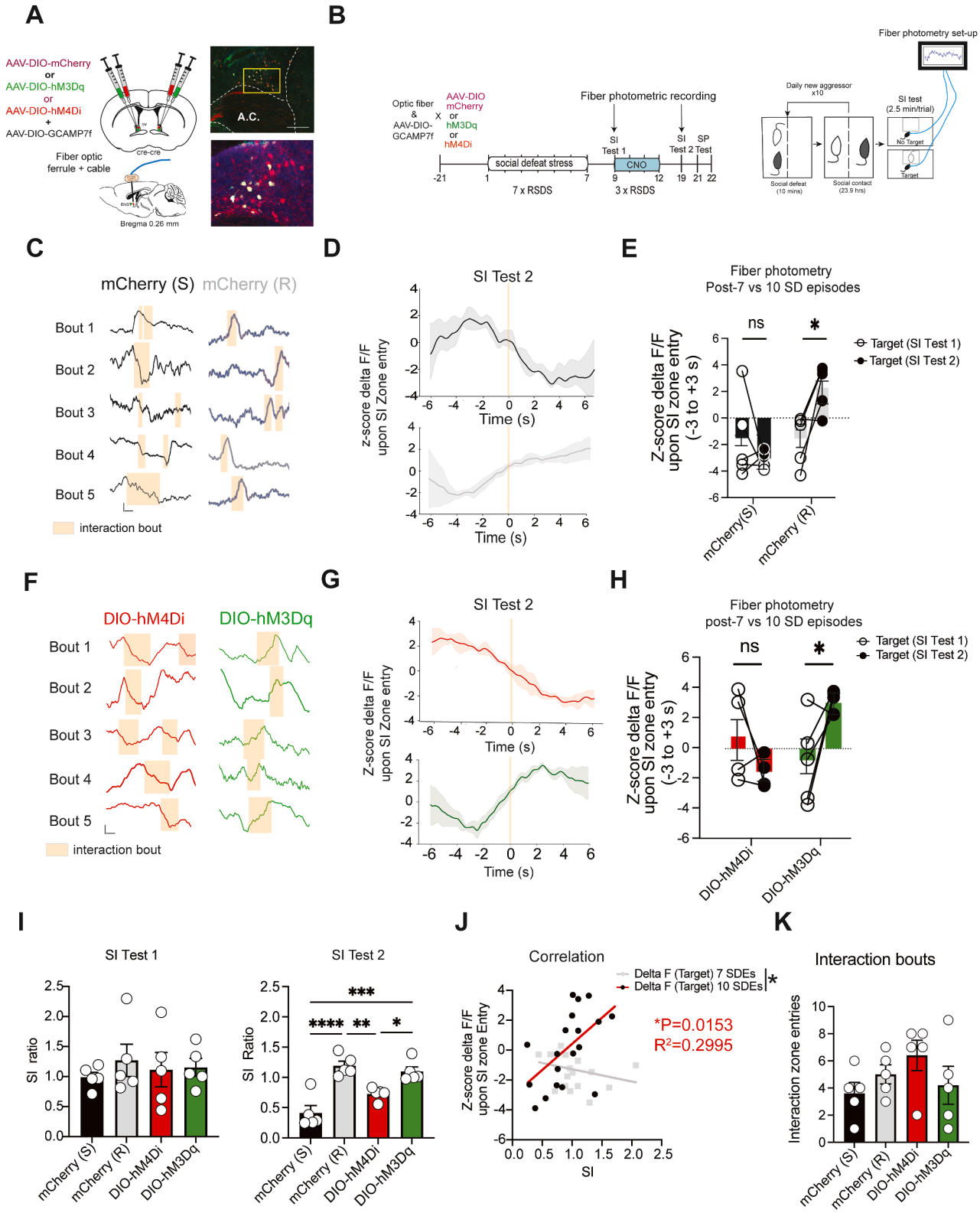

Figure 4. BNSTovCRF calcium-dynamics encode stress effect on social interaction. **(A)** Viral targeting of the the BNSTov. **(B)** Experimental design of multiplexed chemogenetics with drinking water-CNO delivery and fiber photometry. **(C–F)** Representative calcium recordings of mCherry susceptible (S), mCherry resilient (R), hM3Dq, and hM4Di groups, respectively. The vertical scale bar is equal to a *z* score of 1, and the horizontal scale bar is equal to 10

mice subjected to 7 SDEs (Figure S7A, B) or in the absence of SI (Figure S7C). In contrast, after 10 SDEs, mCherry (R)- and DIO-hM3Dq-injected mice displayed significantly greater neuronal activation upon social contact relative to mCherry (S)- and DIO-hM4Di-injected mice (Figure S7D). Despite the difference in time spent interacting with a novel conspecific, the number of interaction zone entries was not significantly different nor were differences in distance traveled (Figure 4K and Figure S7E). These data suggest that BNSTov^{CRF} neuronal dynamics are differentially altered by stress modulation in accordance with phenotypical display resiliency/susceptibility.

Crfr1 Expression in BNSTov^{CRF} Neurons Mirrors the Behavioral Emergence of Resilience

We observed a stress-induced enhancement in firing rates of BNSTov^{CRF} neurons in resilient mice. To explore the effect of this BNSTov^{CRF} stress modulation on CRF receptor transmission, we used RNAScope in situ hybridization to quantify *Crfr1* and *Crfr2* in accordance with stress history. Mice were subjected to either 7 or 10 daily SDEs, and the BNST and *Crfr1* and *Crfr2* genes were assessed (Figure 5A–C) due to their reported role in mediating stress responses (28,61–63). The percentage of CRFR1-expressing neurons among CRF-expressing neurons was higher in mice subjected to 7 SDEs than in susceptible mice but not significantly different than resilient mice (Figure 5D). In contrast, there were no significant differences in BNSTov neurons co-expressing *Crfr2* and *Crf* messenger RNA (mRNA) across groups of mice (Figure 5E). The overlap between *Crfr1* and *Crf* in the BNST was significantly greater in the oval nucleus than in anterolateral, anteromedial, and ventral subregions of the anterior dorsal BNST (Figure 5C, F).

To explore the role of firing rate changes on gene expression and the development of resiliency, we optogenetically stimulated BNSTov^{CRF} neurons using transgenic *Crf-Cre*::ai32 mice, which express ChR2 in *Crf*-containing neurons (64) (Figure 5G). Stimulation frequency of 5 Hz was used to mirror the average firing rate observed in the spontaneous firing rate of resilient mice (Figure 2D). Mice received 15 minutes of 5-Hz photostimulation of BNSTov^{CRF} neurons following physical stress during SDEs 8 to 10. The compartment divides the aggressor cage in half by a clear plexiglass that allows for continuous sensory cues (Figure 5H, I). Photostimulation of *Crf*::ChR2 mice led to a significantly higher SI ratio and greater percentage resilient than *Crf*::tdTomato mice (89% vs. 33%) when stimulated during SDEs 8 to 10 (Figure 5J). Surprisingly, *Crf*::ChR2 mice that received photostimulation but were not subjected to SDEs 8 to 10 showed a significant decrease in the SI ratio and 100% of the mice, becoming susceptible (0/6, SI $\geq$ 1.0) (Figure 5J). Photostimulation paired with SDEs 8 to 10 increased the percentage of cells co-expressing *Crfr1* mRNA in CRF^{+} neurons relative to mice that experienced photostimulation in the absence of additional stress (Figure 5K, L). Additionally, we obtained slice preparation from the optogenetically induced resilient mice and performed cell-attached single-unit recordings from BNSTov ChR2-expressing CRF neurons (Figure S8A). Our recording data showed that optogenetic stimulation reliably induced 2.5, 5, and 10-Hz spike responses as expected (Figure S8B) and interestingly triggered burst firing after the 5-Hz optical stimulation (Figure S8C, D). Importantly, bath-applied CRFR1-selective antagonist NBI 27914 significantly decreased the firing rate of tested BNSTov ChR2-expressing CRF neurons (Figure S8E). We have confirmed the correct placement of optical fibers for these experiments (Figure S8F). Optogenetic stimulation in *Crf-Cre*::ai32 mice may activate both BNSTov- localized CRF neurons and CRF^{+} afferent inputs from extra-BNSTov regions. However, results consistent with previous chemogenetic experiments, together with specific optogenetic activation frequency (5 Hz), support the conclusion that the observed effects are primarily mediated by BNSTov^{CRF} neurons. In summary, these data show that maintenance of resiliency requires SDS. BNSTov^{CRF} activation is correlated with the upregulation of *Crfr1* expression in a stress history–dependent manner.

DISCUSSION

The RSDS paradigm was modified to observe the effects of cumulative stress on neuroplasticity in regions critical for mood regulation. Indeed, our work has uncovered a discrete window of neuronal and behavioral plasticity between 7 and 10 SDEs during which susceptible and resilient phenotypes are established. By capturing behavioral, electrophysiological, and in vivo fiber photometric measures during the intra-SDS period, we uncovered the mechanisms underlying the establishment of resilience. We hypothesized that the region would be instrumental in processing contexts associated with social stress. Indeed, we observed that individual differences in stress effects on social behavior are encoded by BNSTov^{CRF} neurons. Prior studies have implicated the overactivation of CRF neurons in the BNST as being prodepressive and anxiogenic (29,38,49,50,52). We observed that Cre-dependent hM3Dq action produced resilient mice only after a certain dose of daily stressors (7 SDEs), suggesting that the BNSTov may be tightly modulated based on stress history. In addition to the difference between cumulative stress and acute stress (65), the heterogeneity of CRF neurons in different subregions of the BNST may explain the correlation between the

seconds. **(D–G)** Representative averaged trace centered around interaction bout for the 4 groups stated above. **(E)** Two-way repeated-measures ANOVA row factor $F_{3,14} = 1.401$; pre- vs. post-CNO $F_{1,14} = 0.8179$; subject $F_{14,14} = 1.195$; row $\times$ SI test 1/SI test 2, $F_{3,14} = 9.343$, $^{**}p < .01$. Sidak's post hoc test, susceptible vs. resilient, $p = .137$ vs. $^{*}p = .05$, respectively ($n = 4$ mice/group). **(H)** hM4Di vs. hM3Dq, $p = .3069$ vs. $^{*}p < .05$, respectively ($n = 4$–5 mice/group). **(I)** SI test 1 social interaction test. One-way ANOVA $F_{3,16} = 0.291$, $p = .8308$ ($n = 5$ mice/group). SI test 2 social interaction test, one-way ANOVA $F_{3,16} = 17.83$, $^{****}p < .0001$; Tukey's post hoc test, susceptible vs. resilient, $^{****}p < .0001$; susceptible vs. hM3Dq, $^{***}p < .001$; susceptible vs. hM4Di, $p = .0762$; resilient vs. hM3Dq, $p = .8506$; resilient vs. HM4Di, $^{**}p < .01$; hM3Dq vs. hM4Di, $^{*}p < .05$ ($n = 5$ mice/group). **(J)** Correlation of the SI ratio and *z*-score delta F/F upon social entry, simple linear regression pre-CNO $F_{1,15} = 0.7674$, $p = .3948$; SI test 2 $F_{1,17} = 7.268$, $^{*}p < .05$. Intersection of lines, $F_{1,32} = 6.896$, $^{*}p < .05$ ($n = 18$ mice). **(K)** Number of social interaction bouts, one-way ANOVA $F_{3,16} = 1.346$, $p = .2949$ ($n = 5$ mice/group). All data represent mean $\pm$ SEM. $^{*}p < .05$, $^{**}p < .01$, $^{***}p < .001$, $^{****}p < .0001$. ANOVA, analysis of variance; BNSTov, oval nucleus of the bed nucleus of the stria terminalis; CNO, clozapine *N*-oxide; ns, not significant; RSDS, repeated social defeat stress; SDE, social defeat episode; SI, social interaction; SP, sucrose preference.

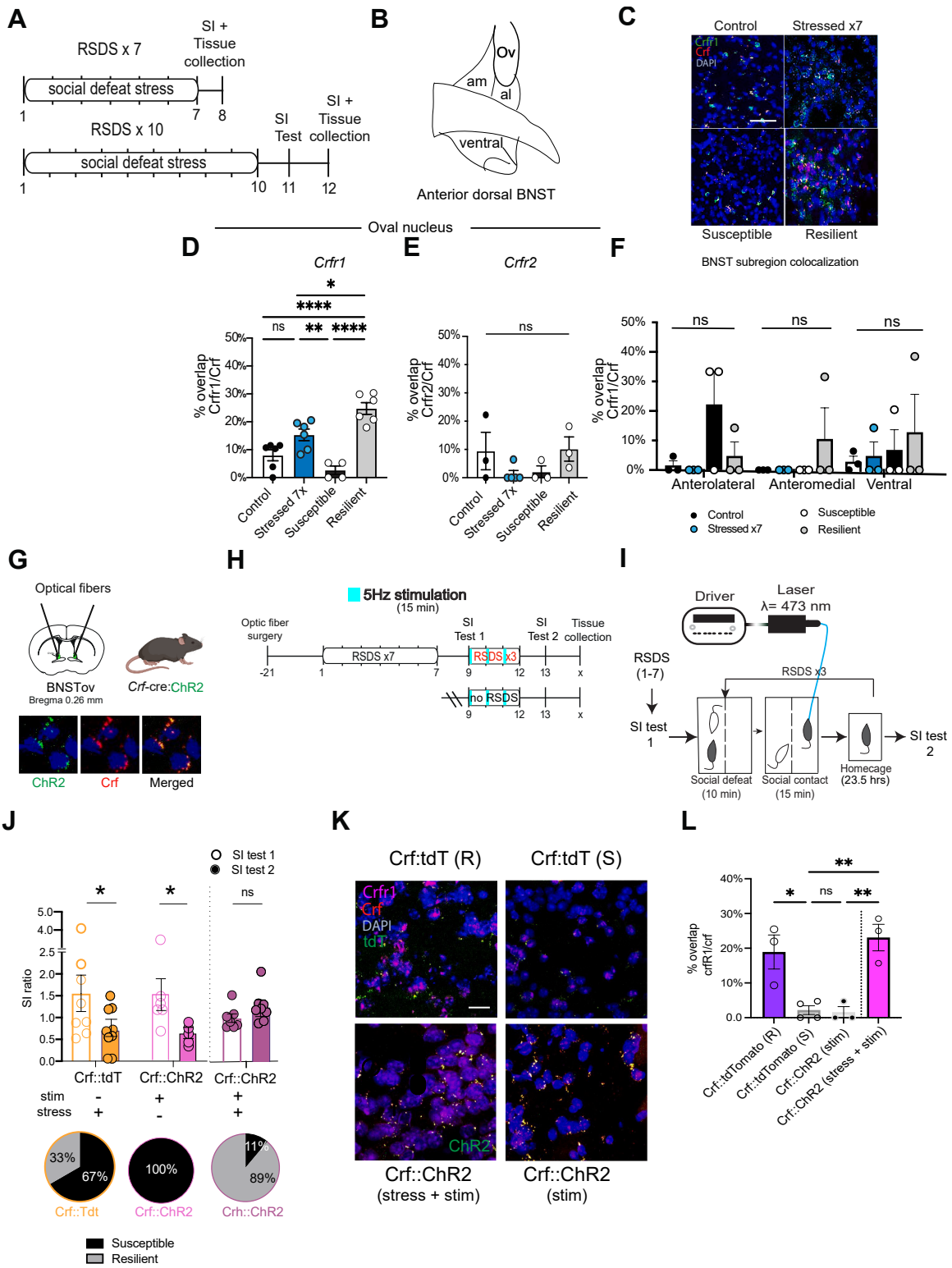

Figure 5. BNSTov *Crfr1* is associated with the emergence of resiliency. **(A)** Experimental timeline of RNAScope in situ hybridization of mice that underwent social defeat stress. **(B)** Representative images of control, stressed ×7, susceptible, and resilient. 20× magnification; scale bar 0.64 mm. **(C)** Schematic of anterior dorsal BNST. **(D)** *Crfr1* mRNA colocalization, 1-way ANOVA $F_{3,18} = 20.91$, ****$p < .0001$; Tukey's post hoc test, control vs. stressed ×7, $p = .0701$; control vs. susceptible, $p = .3336$; control vs. resilient, ****$p < .0001$; stressed ×7 vs. susceptible, **$p < .01$; stressed ×7 vs. resilient, *$p < .05$; susceptible vs.

activation of this type of neuron and resilience, while previous results have shown that activation of $BNST^{CRF}$ neurons reduces effortful motivation behaviors of mice (66). Our current study supports that accumulation of stress (SDE) to 7 days upregulates the activity of BNSTov CRF^+ neurons and develops a resilience phenotype. It suggests that resilience is not a completely preexisting phenotype. It develops during accumulation of chronic stress and depends on stress experience. This is highly consistent with previous demonstrations that resilience is a status achieved by active regulation of genes and ion channel functions in this group more than in susceptible animals (18,19,67–72). CRF neurons have been observed to influence the salience of stressful contexts according to stress exposure (22,25,63,69,73). We observed *Crfr1* mRNA expression in CRF (and not neighboring CRF^-) neurons, suggesting that stress works as a proresilient agent based on stress history. This is contrary to what has been observed, namely that CRFR1 has been found largely on non-CRF neurons in the BNST (73,74).

CRFR1 is selectively activated in the context of ongoing stress, serving as a coincidence detector (75). Chronic stress has been shown to shift the connectivity of local CRF^+ neurons from CRF^+-CRF^- to a larger percentage of CRF^+-CRF^+ cells (76). Studies using prolonged overactivation (over weeks to months) of CRF activity have yielded antidepressant and anxiolytic results (27,32,33). By optogenetically activating $BNSTov^{CRF}$ neurons, we observed an increase in CRFR1 expression. Although correlative, this exquisite regulation of CRFR1 according to stress history and at times demonstrating an opposing effect on depressive-like behavior may underlie why clinical trials of CRFR1 antagonists for MDD have been met with variable success (62,77–79). Additionally, given that the BNST is a sexually dimorphic region, exploration of sex differences is warranted. While not used in this study, there have been additional female SDS models that have shown modest effects regarding susceptible/resilient phenotypes (36,80). Further studies are warranted to select the best alternate female SDS model to adequately compare results from the models.

Conclusions

Stress-sensitive regions such as the BNST have been found to be of critical importance in stress coping and reactivity (81–83). Stress resilience has long been considered a response separate from or in the absence of stimuli that gives rise to stress susceptibility, mediated by parallel circuits or cell types in a particular brain region (12,13,84). Here, we observed that activity dynamics of CRF neurons can shape and influence resiliency to stress, potentially through (auto)regulation of *Crfr1* mRNA. Previous work has shown that resiliency is influenced by dopaminergic VTA neurons in the nucleus accumbens (NAc) (27), in part through the actions of brain-derived neurotrophic factor (BDNF) (19,44,85). CRF peptide has been important for BDNF release in the NAc as a stress-coincidence sensor (18), but the sources of CRF important for altering stress effect on social and hedonic behavior have not been extensively characterized. While long-range GABAergic (gamma-aminobutyric acidergic) BNST neurons projecting to the VTA have been shown to influence reward and anxiety-like behavior (51,86–89), the extent to which these neurons constitute the BNSTov population remains unclear. The BNST also sends projections to the dorsal raphe, lateral and paraventricular hypothalamus, and ventrolateral periaqueductal gray (25,29–31,41,81,90–92), among others, modulation of which has been linked to stress on affect and social motivation. In this way, the BNST acts as a node for integrating information regarding stress history and determining socio-affective outcomes according, possibly due to CRFR1 receptor dynamics occurring on CRF neurons of the oval nucleus, thereby shaping the long-lasting outcome of resiliency. Our study highlights a previously unknown mechanism by which the BNST encodes cumulative social stress and effectuates susceptible or resilient outcomes. Importantly, there are currently no Food and Drug Administration–approved drugs aimed at preventing a depressive episode from occurring. By targeting mechanisms involved in establishing resiliency, the possibility may exist to therapeutically leverage windows of plasticity to effectuate resilience and evade the development of MDD.

ACKNOWLEDGMENTS AND DISCLOSURES

This work was supported by the National Institutes of Health (Grant No. R01MH072908 [to DGR and LJY], Grant Nos. R01MH1206387 and R21MH112081 [to M-HH; principal investigator, Scott J. Russo], Grant No. F31MH114624 [to SEH], and Grant No. P51 OD011132), the National Key R&D Program of 1034 China (Grant Nos. 2021ZD0202900 and 2021ZD0202902), the Research Fund for International Senior Scientists (Grant No. T2250710685), the Shenzhen Natural Science Foundation (Grant Nos. JCYJ20220818101600001 and CYJ20241202125015020), the Shenzhen Key Laboratory of Precision Diagnosis and Treatment of Depression (Grant No. ZDSYS20220606100606014), the Shenzhen Medical Research Fund (Grant No. SMRF B2303012), and the Science and Technology Research and Development Foundation of Shenzhen (High-level Talent Innovation and Entrepreneurship Plan of Shenzhen Team Funding) (Grant No. KQTD20221101093608028 [to M-HH, FL, and XY]).

We thank Dr. Sarah Montgometry for generous sharing for input on the manuscript. We thank Dr. Scott J. Russo and Dr. Long Li for lending viral

resilient, ****$p < .0001$ (n = 4–6 BNST brain samples). **(E)** *Crfr2* mRNA colocalization, one-way ANOVA $F_{3,10} = 1.790$, $p = .2166$ (n = 3 BNST brain samples). **(F)** RNAScope BNST subregion comparison, two-way ANOVA interaction $F_{6,24} = 1.057$, $p = .4147$; row factor $F_{2,24} = 0.6092$, $p = .5520$; column factor $F_{3,24} = 1.549$, $p = .2275$ (n = 3 BNST brain samples). **(G)** Viral injection site. **(H)** Experimental timeline. **(I)** Optogenetic and social behavioral setup. **(J)** Optogenetics social interaction, two-way ANOVA interaction $F_{1,28} = 5.059$, *$p < .05$; row factor $F_{1,28} = 1.061e\text{-}005$, $p = .9974$; column factor $F_{1,28} = 1.419$, $p = .2436$. Sidak's post hoc test, *Crf*::tdT, *$p < .05$; *Crf*::ChR2, $p = .7233$ (n = 7–9 mice/group). Optogenetic manipulation unpaired t test, *Crf*::tdT, $t_{40} = 2.556$, *$p < .05$ (n = 8–9 mice); *Crf*::ChR2, $t_{40} = 0.7758$, $p = .442457$ (n = 8–9 mice); *Crf*::ChR2, $t_{40} = 2.369$, *$p < .05$ (n = 6 mice). Holm-Sidak method for multiple comparisons. **(K)** Representative image, scale bar 0.64 mm. **(L)** Optogenetics- RNAScope experiment. One-way ANOVA $F_{3,9} = 13.53$, **$p < .01$. Tukey's post hoc test, *Crf*::ChR2 (stress + stim) vs. *Crf*::tdT (resilient), $p = .7872$; *Crf*::ChR2 (stress + stim) vs. *Crf*::tdTomato (S), **$p < .01$; *Crf*::ChR2 (stress + stim) vs. *Crf*::chR2 (stim), **$p < .01$; *Crf*::tdTomato (R) vs. *Crf*::tdTomato (S), *$p < .05$; *Crf*::tdTomato (R) vs. *Crf*::ChR2 (stim), *$p < .05$; *Crf*::tdTomato (S) vs. *Crf*::ChR2 (stim), $p = .9988$. All data represent mean ± SEM. *$p < .05$, **$p < .01$, ***$p < .001$, ****$p < .0001$. ANOVA, analysis of variance; BNSTov, oval nucleus of the bed nucleus of the stria terminalis; mRNA, messenger RNA; ns, not significant.

constructs for behavioral validation. We thank the animal care staff at ISMMS for the animal care staff and technical support.

A previous version of this article was published as a preprint on bioRxiv: https://doi.org/10.1101/2022.10.16.512419.

All source data for this manuscript and MATLAB code used to analyze photometry data are available upon request.

HSM receives consulting and intellectual property licensing fees from Abbott Neuromodulation. All other authors report no biomedical financial interests or potential conflicts of interest.

ARTICLE INFORMATION

From the Center for Translational Social Neuroscience, Yerkes National Primate Research Center, Department of Psychiatry and Behavioral Sciences, Emory University, Atlanta, Georgia (SEH, HSS, AM, DGR, LJY); Neuroscience Graduate Program, Emory University, Atlanta, Georgia (SEH); Department of Pharmacological Sciences, Icahn School of Medicine at Mount Sinai, New York, New York (SEH, CM, M-HH); Department of Psychiatry and Behavioral Sciences, Stanford University School of Medicine, Stanford, California (SEH); Nash Family Department of Neuroscience and Friedman Brain Institute, Icahn School of Medicine at Mount Sinai, New York, New York (AL, RLC, M-HH); Department of Mental Health and Public Health, Faculty of Life and Health Sciences, Shenzhen University of Advanced Technology, Shenzhen, Guangdong, China (FL, XY, M-HH); The Brain Cognition and Brain Disease Institute, Shenzhen Institute of Advanced Technology, Chinese Academy of Sciences, Shenzhen, Guangdong, China (FL, XY, M-HH); Nash Family Center for Advanced Circuit Therapeutics, Icahn School of Medicine at Mount Sinai, New York, New York (MFA, KR, HSM); Department of Neurobiology, Harvard Medical School, Kempner Institutes for the Study of Natural and Artificial Intelligence, Boston, Massachusetts (KR); and Department of Anatomy and Neurobiology, University of Maryland, Baltimore School of Medicine, Baltimore, Maryland (BJ).

AL and HSS contributed equally to this work.

Address correspondence to Ming-Hu Han, Ph.D., at ming-hu.han@mssm.edu or hanmh@siat.ac.cn.

Received Apr 16, 2025; revised Oct 9, 2025; accepted Oct 14, 2025.

Supplementary material cited in this article is available online at https://doi.org/10.1016/j.bpsgos.2025.100656.

REFERENCES

1. Veer IM, Riepenhausen A, Zerban M, Wackerhagen C, Puhlmann LMC, Engen H, *et al.* (2021): Psycho-social factors associated with mental resilience in the Corona lockdown. Transl Psychiatry 11:67.
2. Post RM (1992): Transduction of psychosocial stress into the neurobiology of recurrent affective disorder. Am J Psychiatry 149:999–1010.
3. Gold PW (2013): Evidence that stress per se has a role in the precipitation and natural history of depressive illness. Mol Psychiatry 18:954–956.
4. Kendler KS, Karkowski LM, Prescott CA (1999): Causal relationship between stressful life events and the onset of major depression. Am J Psychiatry 156:837–841.
5. Barthas F, Hu MY, Siniscalchi MJ, Ali F, Mineur YS, Picciotto MR, Kwan AC (2020): Cumulative effects of social stress on reward-guided actions and prefrontal cortical activity. Biol Psychiatry 88:541–553.
6. Kudryavtseva NN, Bakshtanovskaya IV, Koryakina LA (1991): Social model of depression in mice of C57BL/6J strain. Pharmacol Biochem Behav 38:315–320.
7. Laine MA, Sokolowska E, Dudek M, Callan S-A, Hyytiä P, Hovatta I (2017): Brain activation induced by chronic psychosocial stress in mice. Sci Rep 7:15061.
8. Drysdale AT, Grosenick L, Downar J, Dunlop K, Mansouri F, Meng Y, *et al.* (2017): Resting-state connectivity biomarkers define neurophysiological subtypes of depression. Nat Med 23:28–38.
9. Samuels BA, Leonardo ED, Gadient R, Williams A, Zhou J, David DJ, *et al.* (2011): Modeling treatment-resistant depression. Neuropharmacology 61:408–413.
10. Franklin TB, Saab BJ, Mansuy IM (2012): Neural mechanisms of stress resilience and vulnerability. Neuron 75:747–761.
11. Russo SJ, Murrough JW, Han M-H, Charney DS, Nestler EJ (2012): Neurobiology of resilience. Nat Neurosci 15:1475–1484.
12. Karatsoreos IN, McEwen BS (2011): Psychobiological allostasis: Resistance, resilience and vulnerability. Trends Cogn Sci 15:576–584.
13. Golden SA, Covington HE, Berton O, Russo SJ (2011): A standardized protocol for repeated social defeat stress in mice. Nat Protoc 6:1183–1191.
14. Martinez M, Phillips PJ, Herbert J (1998): Adaptation in patterns of c-fos expression in the brain associated with exposure to either single or repeated social stress in male rats. Eur J Neurosci 10:20–33.
15. Laine MA, Trontti K, Misiewicz Z, Sokolowska E, Kulesskaya N, Heikkinen A, *et al.* (2018): Genetic control of myelin plasticity after chronic psychosocial stress. eNeuro 5:ENEURO.0166-18.2018.
16. Markham CM, Norvelle A, Huhman KL (2009): Role of the bed nucleus of the stria terminalis in the acquisition and expression of conditioned defeat in Syrian hamsters. Behav Brain Res 198:69–73.
17. Gururajan A, Bastiaanssen TFS, Ventura Silva AP, Moloney GM, Cryan JF (2022): The impact of psychosocial defeat stress on the bed nucleus of the stria terminalis transcriptome in adult male mice. Eur J Neurosci 55:67–77.
18. Walsh JJ, Friedman AK, Sun H, Heller EA, Ku SM, Juarez B, *et al.* (2014): Stress and CRF gate neural activation of BDNF in the mesolimbic reward pathway. Nat Neurosci 17:27–29.
19. Krishnan V, Han M-H, Graham DL, Berton O, Renthal W, Russo SJ, *et al.* (2007): Molecular adaptations underlying susceptibility and resistance to social defeat in brain reward regions. Cell 131:391–404.
20. Matsuda S, Peng H, Yoshimura H, Wen TC, Fukuda T, Sakanaka M (1996): Persistent c-fos expression in the brains of mice with chronic social stress. Neurosci Res 26:157–170.
21. Berton O, McClung CA, Dileone RJ, Krishnan V, Renthal W, Russo SJ, *et al.* (2006): Essential role of BDNF in the mesolimbic dopamine pathway in social defeat stress. Science 311:864–868.
22. Waraczynski M (2016): Toward a systems-oriented approach to the role of the extended amygdala in adaptive responding. Neurosci Biobehav Rev 68:177–194.
23. Flanigan ME, Kash TL (2022): Coordination of social behaviors by the bed nucleus of the stria terminalis. Eur J Neurosci 55:2404–2420.
24. Lebow MA, Chen A (2016): Overshadowed by the amygdala: The bed nucleus of the stria terminalis emerges as key to psychiatric disorders. Mol Psychiatry 21:450–463.
25. Daniel SE, Rainnie DG (2016): Stress modulation of opposing circuits in the bed nucleus of the stria terminalis. Neuropsychopharmacology 41:103–125.
26. Jennings JH, Sparta DR, Stamatakis AM, Ung RL, Pleil KE, Kash TL, Stuber GD (2013): Distinct extended amygdala circuits for divergent motivational states. Nature 496:224–228.
27. Dedic N, Kühne C, Jakovcevski M, Hartmann J, Genewsky AJ, Gomes KS, *et al.* (2018): Chronic CRH depletion from GABAergic, long-range projection neurons in the extended amygdala reduces dopamine release and increases anxiety. Nat Neurosci 21:803–807.
28. Chen Y, Molet J, Gunn BG, Ressler K, Baram TZ (2015): Diversity of reporter expression patterns in transgenic mouse lines targeting corticotropin-releasing hormone-expressing neurons. Endocrinology 156:4769–4780.
29. Dabrowska J, Martinon D, Moaddab M, Rainnie DG (2016): Targeting corticotropin-releasing factor projections from the oval nucleus of the bed nucleus of the stria terminalis using cell-type specific neuronal tracing studies in mouse and rat brain. J Neuroendocrinol 28.
30. Matthews GA, Nieh EH, Vander Weele CM, Halbert SA, Pradhan RV, Yosafat AS, *et al.* (2016): Dorsal raphe dopamine neurons represent the experience of social isolation. Cell 164:617–631.
31. Marcinkiewcz CA, Mazzone CM, D'Agostino G, Halladay LR, Hardaway JA, DiBerto JF, *et al.* (2016): Serotonin engages an anxiety and fear-promoting circuit in the extended amygdala. Nature 537:97–101.
32. Regev L, Neufeld-Cohen A, Tsoory M, Kuperman Y, Getselter D, Gil S, Chen A (2011): Prolonged and site-specific over-expression of corticotropin-releasing factor reveals differential roles for extended amygdala nuclei in emotional regulation. Mol Psychiatry 16:714–728.
33. Sink KS, Walker DL, Freeman SM, Flandreau EI, Ressler KJ, Davis M (2013): Effects of continuously enhanced corticotropin releasing factor

expression within the bed nucleus of the stria terminalis on conditioned and unconditioned anxiety. Mol Psychiatry 18:308–319.
34. Konishi S-i, Kasagi Y, Katsumata H, Minami S, Imaki T (2003): Regulation of corticotropin-releasing factor (CRF) type-1 receptor gene expression by CRF in the hypothalamus. Endocr J 50:21–36.
35. Jasnow AM, Banks MC, Owens EC, Huhman KL (1999): Differential effects of two corticotropin-releasing factor antagonists on conditioned defeat in male Syrian hamsters (Mesocricetus auratus). Brain Res 846:122–128.
36. Zhang N, Zhao S, Ma YQ, Xiao ZX, Xue B, Dong Y, *et al.* (2024): Hyperexcitation of ovBNST CRF neurons during stress contributes to female-biased expression of anxiety-like avoidance behaviors. Sci Adv 10:eadk7636.
37. Avery SN, Clauss JA, Blackford JU (2016): The human BNST: Functional role in anxiety and addiction. Neuropsychopharmacology 41:126–141.
38. Kim S-Y, Adhikari A, Lee SY, Marshel JH, Kim CK, Mallory CS, *et al.* (2013): Diverging neural pathways assemble a behavioural state from separable features in anxiety. Nature 496:219–223.
39. Rodríguez-Sierra OE, Goswami S, Turesson HK, Pare D (2016): Altered responsiveness of BNST and amygdala neurons in trauma-induced anxiety. Transl Psychiatry 6:e857.
40. Ventura-Silva AP, Pêgo JM, Sousa JC, Marques AR, Rodrigues AJ, Marques F, *et al.* (2012): Stress shifts the response of the bed nucleus of the stria terminalis to an anxiogenic mode. Eur J Neurosci 36:3396–3406.
41. Giardino WJ, Eban-Rothschild A, Christoffel DJ, Li S-B, Malenka RC, de Lecea L (2018): Parallel circuits from the bed nuclei of stria terminalis to the lateral hypothalamus drive opposing emotional states. Nat Neurosci 21:1084–1095.
42. Duvarci S, Bauer EP, Paré D (2009): The bed nucleus of the stria terminalis mediates inter-individual variations in anxiety and fear. J Neurosci 29:10357–10361.
43. Duque-Wilckens N, Torres LY, Yokoyama S, Minie VA, Tran AM, Petkova SP, *et al.* (2020): Extrahypothalamic oxytocin neurons drive stress-induced social vigilance and avoidance. Proc Natl Acad Sci U S A 117:26406–26413.
44. Wook Koo J, Labonté B, Engmann O, Calipari ES, Juarez B, Lorsch Z, *et al.* (2016): Essential role of mesolimbic brain-derived neurotrophic factor in chronic social stress-induced depressive behaviors. Biol Psychiatry 80:469–478.
45. Cao J-L, Covington HE, Friedman AK, Wilkinson MB, Walsh JJ, Cooper DC, *et al.* (2010): Mesolimbic dopamine neurons in the brain reward circuit mediate susceptibility to social defeat and antidepressant action. J Neurosci 30:16453–16458.
46. Morel C, Montgomery SE, Li L, Durand-de Cuttoli R, Teichman EM, Juarez B, *et al.* (2022): Midbrain projection to the basolateral amygdala encodes anxiety-like but not depression-like behaviors. Nat Commun 13:1532.
47. Kumar S, Hultman R, Hughes D, Michel N, Katz BM, Dzirasa K (2014): Prefrontal cortex reactivity underlies trait vulnerability to chronic social defeat stress. Nat Commun 5:4537.
48. Dabrowska J, Hazra R, Guo J-D, Li C, Dewitt S, Xu J, *et al.* (2013): Striatal-enriched protein tyrosine phosphatase-STEPs toward understanding chronic stress-induced activation of corticotrophin releasing factor neurons in the rat bed nucleus of the stria terminalis. Biol Psychiatry 74:817–826.
49. Hu P, Liu J, Maita I, Kwok C, Gu E, Gergues MM, *et al.* (2020): Chronic stress induces maladaptive behaviors by activating corticotropin-releasing hormone signaling in the mouse oval bed nucleus of the stria terminalis. J Neurosci 40:2519–2537.
50. Daniel SE, Menigoz A, Guo J, Ryan SJ, Seth S, Rainnie DG (2019): Chronic stress induces cell type-selective transcriptomic and electrophysiological changes in the bed nucleus of the stria terminalis. Neuropharmacology 150:80–90.
51. Wanat MJ, Bonci A, Phillips PEM (2013): CRF acts in the midbrain to attenuate accumbens dopamine release to rewards but not their predictors. Nat Neurosci 16:383–385.
52. Salimando GJ, Hyun M, Boyt KM, Winder DG (2020): BNST GluN2D-containing NMDA receptors influence anxiety- and depressive-like behaviors and ModulateCell-specific excitatory/inhibitory synaptic balance. J Neurosci 40:3949–3968.
53. Hartley ND, Gaulden AD, Báldi R, Winters ND, Salimando GJ, Rosas-Vidal LE, *et al.* (2019): Dynamic remodeling of a basolateral-to-central amygdala glutamatergic circuit across fear states. Nat Neurosci 22:2000–2012.
54. Sanford CA, Soden ME, Baird MA, Miller SM, Schulkin J, Palmiter RD, *et al.* (2017): A central amygdala CRF circuit facilitates learning about weak threats. Neuron 93:164–178.
55. Rodríguez-Sierra OE, Turesson HK, Pare D (2013): Contrasting distribution of physiological cell types in different regions of the bed nucleus of the stria terminalis. J Neurophysiol 110:2037–2049.
56. Gungor NZ, Paré D (2016): Functional heterogeneity in the bed nucleus of the stria terminalis. J Neurosci 36:8038–8049.
57. Zhan J, Komal R, Keenan WT, Hattar S, Fernandez DC (2019): Non-invasive strategies for chronic manipulation of DREADD-controlled neuronal activity. J Vis Exp 150.
58. Schalbetter SM, Mueller FS, Scarborough J, Richetto J, Weber-Stadlbauer U, Meyer U, Notter T (2021): Oral application of clozapine-N-oxide using the micropipette-guided drug administration (MDA) method in mouse DREADD systems. Lab Anim (NY) 50:69–75.
59. Wess J, Nakajima K, Jain S (2013): Novel designer receptors to probe GPCR signaling and physiology. Trends Pharmacol Sci 34:385–392.
60. Walker DL, Miles LA, Davis M (2009): Selective participation of the bed nucleus of the stria terminalis and CRF in sustained anxiety-like versus phasic fear-like responses. Prog Neuropsychopharmacol Biol Psychiatry 33:1291–1308.
61. Tran L, Schulkin J, Greenwood-Van Meerveld B (2014): Importance of CRF receptor-mediated mechanisms of the bed nucleus of the stria terminalis in the processing of anxiety and pain. Neuropsychopharmacology 39:2633–2645.
62. Lee Y, Fitz S, Johnson PL, Shekhar A (2008): Repeated stimulation of CRF receptors in the BNST of rats selectively induces social but not panic-like anxiety. Neuropsychopharmacology 33:2586–2594.
63. Dedic N, Kühne C, Gomes KS, Hartmann J, Ressler KJ, Schmidt MV, Deussing JM (2019): Deletion of CRH from GABAergic forebrain neurons promotes stress resilience and dampens stress-induced changes in neuronal activity. Front Neurosci 13:986.
64. Wang Y, Hu P, Shan Q, Huang C, Huang Z, Chen P, *et al.* (2021): Single-cell morphological characterization of CRH neurons throughout the whole mouse brain. BMC Biol 19:47.
65. Snyder AE, Salimando GJ, Winder DG, Silberman Y (2019): Chronic intermittent ethanol and acute stress similarly modulate BNST CRF neuron activity via noradrenergic signaling. Alcohol Clin Exp Res 43:1695–1701.
66. Maita I, Bazer A, Chae K, Parida A, Mirza M, Sucher J, *et al.* (2024): Chemogenetic activation of corticotropin-releasing factor-expressing neurons in the anterior bed nucleus of the stria terminalis reduces effortful motivation behaviors. Neuropsychopharmacology 49:377–385.
67. Chen P, Lou S, Huang ZH, Wang Z, Shan QH, Wang Y, *et al.* (2020): Prefrontal cortex corticotropin-releasing factor neurons control behavioral style selection under challenging situations. Neuron 106:301–315.e7.
68. Elliott E, Ezra-Nevo G, Regev L, Neufeld-Cohen A, Chen A (2010): Resilience to social stress coincides with functional DNA methylation of the Crf gene in adult mice. Nat Neurosci 13:1351–1353.
69. Lemos JC, Wanat MJ, Smith JS, Reyes BAS, Hollon NG, Van Bockstaele EJ, *et al.* (2012): Severe stress switches CRF action in the nucleus accumbens from appetitive to aversive. Nature 490:402–406.
70. Zhang HX, Chaudhury D, Nectow AR, Friedman AK, Zhang S, Juarez B, *et al.* (2019): α1- and β3-adrenergic receptor-mediated mesolimbic homeostatic plasticity confers resilience to social stress in susceptible mice. Biol Psychiatry 85:226–236.
71. Friedman AK, Walsh JJ, Juarez B, Ku SM, Chaudhury D, Wang J, *et al.* (2014): Enhancing depression mechanisms in midbrain dopamine neurons achieves homeostatic resilience. Science 344:313–319.
72. Bagot RC, Cates HM, Purushothaman I, Lorsch ZS, Walker DM, Wang J, *et al.* (2016): Circuit-wide transcriptional profiling reveals brain region-specific gene networks regulating depression susceptibility. Neuron 90:969–983.
73. Dabrowska J, Hazra R, Guo J-D, Dewitt S, Rainnie DG (2013): Central CRF neurons are not created equal: Phenotypic differences in CRF-

containing neurons of the rat paraventricular hypothalamus and the bed nucleus of the stria terminalis. Front Neurosci 7:156.
74. Justice NJ, Yuan ZF, Sawchenko PE, Vale W (2008): Type 1 corticotropin-releasing factor receptor expression reported in BAC transgenic mice: Implications for reconciling ligand-receptor mismatch in the central corticotropin-releasing factor system. J Comp Neurol 511:479–496.
75. Ramot A, Jiang Z, Tian J-B, Nahum T, Kuperman Y, Justice N, Chen A (2017): Hypothalamic CRFR1 is essential for HPA axis regulation following chronic stress. Nat Neurosci 20:385–388.
76. Partridge JG, Forcelli PA, Luo R, Cashdan JM, Schulkin J, Valentino RJ, Vicini S (2016): Stress increases GABAergic neurotransmission in CRF neurons of the central amygdala and bed nucleus stria terminalis. Neuropharmacology 107:239–250.
77. Spierling SR, Zorrilla EP (2017): Don't stress about CRF: Assessing the translational failures of CRF1antagonists. Psychopharmacology 234:1467–1481.
78. Waters RP, Rivalan M, Bangasser DA, Deussing JM, Ising M, Wood SK, *et al.* (2015): Evidence for the role of corticotropin-releasing factor in major depressive disorder. Neurosci Biobehav Rev 58:63–78.
79. Reul JMHM, Holsboer F (2002): Corticotropin-releasing factor receptors 1 and 2 in anxiety and depression. Curr Opin Pharmacol 2:23–33.
80. Uchida K, Otsuka H, Morishita M, Tsukahara S, Sato T, Sakimura K, Itoi K (2019): Correction to: Female-biased sexual dimorphism of corticotropin-releasing factor neurons in the bed nucleus of the stria terminalis. Biol Sex Differ 10:10.
81. Johnson SB, Emmons EB, Anderson RM, Glanz RM, Romig-Martin SA, Narayanan NS, *et al.* (2016): A basal forebrain site coordinates the modulation of endocrine and behavioral stress responses via divergent neural pathways. J Neurosci 36:8687–8699.
82. Crestani CC, Alves FHF, Correa FMA, Guimarães FS, Joca SRL (2010): Acute reversible inactivation of the bed nucleus of stria terminalis induces antidepressant-like effect in the rat forced swimming test. Behav Brain Funct 6:30.
83. Fiedler D, Sasi M, Blum R, Klinke CM, Andreatta M, Pape HC, Lange MD (2021): Brain-derived neurotrophic factor/tropomyosin receptor kinase B signaling controls excitability and long-term depression in oval nucleus of the BNST. J Neurosci 41:435–445.
84. Cathomas F, Murrough JW, Nestler EJ, Han M-H, Russo SJ (2019): Neurobiology of resilience: Interface between mind and body. Biol Psychiatry 86:410–420.
85. Koo JW, Chaudhury D, Han MH, Nestler EJ (2019): Role of mesolimbic brain-derived neurotrophic factor in depression. Biol Psychiatry 86:738–748.
86. Takahashi D, Asaoka Y, Kimura K, Hara R, Arakaki S, Sakasai K, *et al.* (2019): Tonic suppression of the mesolimbic dopaminergic system by enhanced corticotropin-releasing factor signaling within the bed nucleus of the stria terminalis in chronic pain model rats. J Neurosci 39:8376–8385.
87. Caillé S, Guillem K, Cador M, Manzoni O, Georges F (2009): Voluntary nicotine consumption triggers in vivo potentiation of cortical excitatory drives to midbrain dopaminergic neurons. J Neurosci 29:10410–10415.
88. Silberman Y, Matthews RT, Winder DG (2013): A corticotropin releasing factor pathway for ethanol regulation of the ventral tegmental area in the bed nucleus of the stria terminalis. J Neurosci 33:950–960.
89. Rodaros D, Caruana DA, Amir S, Stewart J (2007): Corticotropin-releasing factor projections from limbic forebrain and paraventricular nucleus of the hypothalamus to the region of the ventral tegmental area. Neuroscience 150:8–13.
90. Dong HW, Petrovich GD, Watts AG, Swanson LW (2001): Basic organization of projections from the oval and fusiform nuclei of the bed nuclei of the stria terminalis in adult rat brain. J Comp Neurol 436:430–455.
91. Maita I, Bazer A, Blackford JU, Samuels BA (2021): Functional anatomy of the bed nucleus of the stria terminalis-hypothalamus neural circuitry: Implications for valence surveillance, addiction, feeding, and social behaviors. Handb Clin Neurol 179:403–418.
92. Kaouane N, Ada S, Hausleitner M, Haubensak W (2021): Dorsal bed nucleus of the stria terminalis-subcortical output circuits encode positive bias in Pavlovian fear and reward. Front Neural Circuits 15: 772512.